ISSN 2616-5880 Vol. 6, Issue 2: 82-91, DOI: 10.25236/AJMC.2025.060211

The Co-polymerization Kinetics and Flocculation Effects of CO_2-Responsive Cationic Polymers

Junyan Zhang[1], Anqi Ming[1,2], Wencong Li[1], Yan Zhong[1,2], Wei Qi[1,2], Yuhan Ma[1,2], Yuxiang Cao[3], Yanyan Liu[1], Haibao Zhang[1], Xiaoxiao Li[1,*]

[1]Key Lab of Photovoltaic and Energy Conservation Materials, Institute of Solid State Physics, Hefei Institutes of Physical Science, Chinese Academy of Sciences, Hefei, 230031, China
[2]University of Science and Technology of China, Hefei, 230026, China
[3]Zhongke Lemei Science and Technology Group Co., Ltd., Emeishan, 614218, China
[*]Corresponding author: lixiaoxiao@rntek.cas.cn

Abstract: *Cationic polymers are promising flocculants for highly efficient solid-liquid separation, because of their tailorable molecular structures, they can realize remarkable ability of adsorbing contaminant. Herein, a novel copolymerization strategy is reported to obtain a well-designed CO_2-responsive cationic copolymer for effective solid-liquid separation. To be specific, a series of novel CO_2-responsive hyamine-based cationic copolymers (CHOPs) with different molecular structures were synthesized via copolymeization reactions between acryloyl oxygen ethyl trimethyl ammonium chloride (DAC), methyl acryloyl oxygen ethyl trimethyl ammonium chloride (DMC), methyl acryl-amide propyl trimethyl ammonium chloride (MAPTAC) and CO_2-responsive monomer dimethyl amino ethyl methacrylate (DMAEMA). The molar ratios of the monomers were optimized and the copolymerization kinetics followed to obtain the best relative molecular weight of CHOPs with good CO_2-responsiveness and flocculation ability. Of note, the tertiary amine groups of CHOPs could be protonated by the reaction with CO_2, leading to positively charged chains on the copolymers for enhanced flocculation ability. Furthermore, the network structure derived from CO_2 bridging between the two tertiary amine groups were conducive to the viscosity improvement and flocculation enhancement. Moreover, DMAEMA and DMC had the best polymerization kinetics, and the obtained P(DMC_1-$DMAEMA_3$) copolymer was found to be the optimized monomer molar ratio and gave the highest relative molecular mass which showed prominent flocculation ability under selected CO_2 import mode (only import in the flocculation system). The unique CO_2 import method facilitated homogenous reaction between the polymer and CO_2 while combing with solid particles to form ionic hydrophilic quaternary ammonium salts, leading to enhanced electrostatic repulsion between the copolymer chains and weakened interaction. As a result, the copolymer chains were more easily extended to improve bridge-effect. Combined with multiple fine particles, they resulted in increased flocculation volume and accelerated sedimentation rate for highly efficient solid-liquid separation.*

Keywords: *cationic polymer, CO_2-responsive, electric neutralization, adsorption bridging effect, solid-liquid separation*

1. Introduction

Solid-liquid separation is essential for sewage and sludge treatment and recycling.[1] It is urgent to explore effective methods for highly efficient solid-liquid separation owing to the increasing demand of reducing waste volume production.[2] As an important method of strengthening solid-liquid separation in the field of sewage treatment, the flocculation can be used to strengthen the primary precipitation of sewage, flotation treatment and secondary precipitation after activated sludge method, and can also be used for tertiary treatment or advanced treatment of sewage.[3] Water-soluble polymers (WPs), such as cationic-based WPs, anionic-based WPs and amphoteric-based WPs, are promising reagents for solid-liquid separation owing to their good ability of flocculation.[4; 5]

Among the WPs, cationic polymers (CPs) with positively charged molecular chains have attracted attention as potential reagents for solid-liquid separation.[6; 7] Due to the electric neutralized effect derived from the positively charged groups, CPs are attracted to negatively charged particles within sewage and sludge, leading to flocculation enhancement.[8] Of note, the molecular structure and the types of functional groups play a critical role in the performance of flocculation. The quaternary ammonium salt

ISSN 2616-5880 Vol. 6, Issue 2: 82-91, DOI: 10.25236/AJMC.2025.060211

cationic polymers have been considered as the most prospective reagents for solid-liquid separation because of their remarkable water solubility and good stability derived from the unique molecular structure and functional groups.[9] Nevertheless, due to the restriction resulting from simplex charge property and linear structure, ordinary quaternary ammonium salt cationic polymers cannot meet the increasingly requirements for effective solid-liquid separation and complicated solid-liquid separation environments.[10] Therefore, the research and development of flocculants with tunable molecular structure are highly desirable for solid-liquid separation in the future.

Stimuli-responsive polymers with tunable molecular structure can exhibit specific reversibly transformation to accommodate the complex environmental changes.[11; 12] Especially, owing to low cost, environmentally friendly and the unique mechanism of CO_2-responsive transformation, the CO_2-responsive cationic polymers (CCPs) have attracted attention of many researchers.[13; 14] The CCPs can be converted to multifunctional ionic polymers via the reversible reaction between responsive functional groups and CO_2, leading to enhanced floc settling performance and dewaterability.[15; 16] Based on this, Liu et al.[17] employed CO_2-responsive mechanism to optimize extracellular polymeric substances for enhanced self-flocculation of solids in solution and brought new enlightenment to carbon-neutral operation of wastewater treatment plants based on the symbiotic biofilm/biogranules system. Besides, the CO_2 can easily be removed as an activator trigger, which means the CCPs can minimize the negative environmental impact, and it is safer and easier to be applied on a large scale compared to strong acid or strong alkaline responsive CPs.[18; 19] However, the practical application of CCPs has been hindered by the unsatisfactory CO_2 responsiveness. Hence, it is critical to construct a molecular unit with effective CO_2 responsiveness into the molecular chain of CCPs.

Research has shown that tertiary amine monomers like dimethyl amino ethyl methacrylate (DMAEMA) are good at enhancing the CO_2-responsiveness due to the fact that their tertiary amine groups are highly sensitive to CO_2.[20-22] Nittala et al.[23] reported that a series of CO_2-responsive hyamine-based cationic polymers (CHOPs) based on DMAEMA and N-isopropyl acrylamide (NIPAM) exhibited enhanced performance of flocculate oil sands mature fine tailings. It is suggested that CO_2 protonates the tertiary amine groups of Poly-DMAEMA and Poly-(DMAEMA-NIPAM) resulting in positively charged chains. Thus, the pH sensitivity of these polymers favored the flocculation of the negatively charged clays in the solution due to charge neutralization. This led to enhanced flocculation and high performance solid-liquid separation. In addition, quaternary ammonium monomers with quaternary ammonium groups and polymerizable olefinic bonds, such as acryloyl oxygen ethyl trimethyl ammonium chloride (DAC), methyl acryloyl oxygen ethyl trimethyl ammonium chloride (DMC), and methyl acryl-amide propyl trimethyl ammonium chloride (MAPTAC), have been employed to obtain cationic polymers for solid-liquid separation. Ming et al. compared the polymerization kinetics of these cationic monomers and found that the kinetics were influenced by electronic effects and steric hindrance of the monomer structure.[24] However, the lack of molecular design and regulation of CO_2-responsiveness hinder further application of DMAEMA based CCPs in solid-liquid separation. Therefore, it is necessary to further design an effective CCPs via molecular design and regulation of CO_2-responsiveness to realize highly efficient solid-liquid separation.[25]

2. Materials and Methods

2.1 Materials

The cationic monomers, acryloyl oxygen ethyl trimethyl ammonium chloride (DAC, 80% w/w), methyl acryloyl oxygen ethyl trimethyl ammonium chloride (DMC, 88% w/w), and methyl acrylamide propyl trimethyl ammonium chloride (MAPTAC, 50% w/w) were purchased from Jiangsu Feymer Technology Co., Ltd. 2,2'-Azobis(2-methylpropionamide)dihydrochloride (AIBA) was purchased from Wako chemical Co., Ltd. Tetrasodium ethylenediaminetetraacetic acid (Na_4EDTA) was purchased from Shanghai Macklin Biochemical Co., Ltd. Potassium bromide (KBr), potassium bromate ($KBrO_3$), 2-(Dimethylamino)ethyl methacrylate (DMAEMA, 80% w/w), potassium iodide (KI), sodium thiosulfate ($Na_2S_2O_3$) analytical titrant, and soluble starch were purchased from Aladdin Reagent (Shanghai) Co., Ltd. Hydrochloric acid (HCl) and sodium chloride (NaCl) were purchased from Sinopharm Chemical Reagent Co., Ltd.

2.2 Copolymer preparation

Refined DAC (…g, …mol), DMC (…g, …mol) and MAPTAC (…g, …mol) were weighed and fed

ISSN 2616-5880 Vol. 6, Issue 2: 82-91, DOI: 10.25236/AJMC.2025.060211

into a 100 mL plastic bottle, and DMAEMA (…g, …mol) was added to the same plastic bottle. This was followed by addition of … ml Na_4EDTA solution (0.1g Na_4EDTA dissolved in 100 mL distilled water to prepare 0.001 g/ml solution), and …ml of distilled water, the bottle with the reaction mixture placed in a water bath preset at 25 ℃. The reaction mixture was purged with nitrogen gas for 20 min and …ml initiator solution AIBA was added under constant agitation. The water bath temperature was consequently raised to 38-48 ℃ (initiation temperature) for 3 h. Once polymerization was initiated, as indicated by an increase in the viscosity of the solution, the reaction temperature was raised to the curing temperature of 60 ℃ and held for 3 h, and finally the gel-like polymer was obtained. The obtained CHOPs were named by P(cationic monomer x-CO_2 monomer y), where x, y are the molar ratios of the monomers. Figure 1A-C illustrates the copolymerization reactions of P(DAC-DMAEMA), P(DMC-DMAEMA), and P(MAPTAC-DMAEMA).

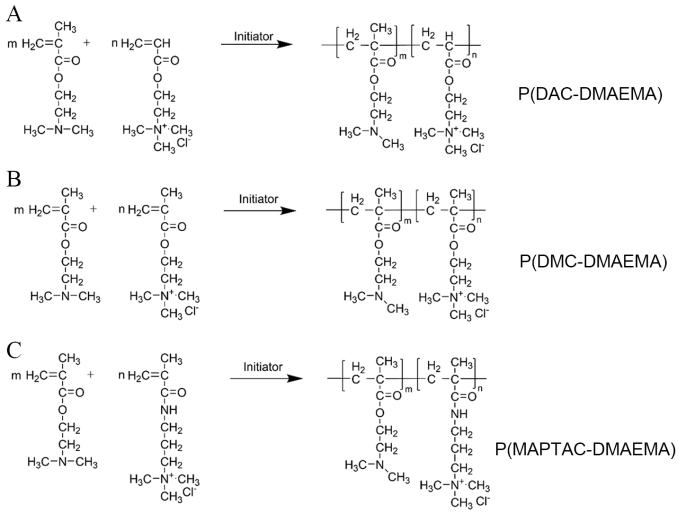

Figure 1. Schematic illustration of the copolymerization of (A) P(DAC-DMAEMA), (B) P(DMC-DMAEMA), and (C) P(MAPTAC-DMAEMA).

2.3 Determination of activation energy (E_a), polymerization kinetics and reactivity ratio

To calculate the polymerization rate, the volume shrinkage factor K was used to determine the monomer conversion rate per unit time. A certain amount of reaction solution was poured into the dilatometer and immersed into a constant temperature water bath. As the polymerization reaction progressed, the volume of the polymerization reaction system gradually shrunk. The beginning of the drop in liquid level indicated the start of the reaction, this was recorded as the initial volume (V_0). This was followed by regular intervals of volume measurements (V_t). After some hours, the reaction was stopped by removing the dilatometer from the water bath, this time was recorded as Ve. The reaction solution was immediately added to 100 mL of cooled deionized water. Then, the monomer conversion rate, α_e, was determined using the potassium bromide-potassium bromate method (Chinese National Standard GB12005.3-89), and the value of K was calculated according to Equation (1).[25]

$$K = \frac{1}{\alpha_e} \times \frac{V_e - V_0}{V_0} \tag{1}$$

The monomer conversion rate corresponding to V_t was calculated according to Equation (2).[25]

$$K = \frac{1}{\alpha_e} \times \frac{V_e - V_0}{V_0} \tag{2}$$

The polymerization rate R_p was determined by plotting a monomer conversion, α, vs time curve the slope of the straight line was used to determine R_p by using Equations 3 and 4.[26]

$$R_p = -\frac{d[M]}{dt} = [M_0]\frac{d\alpha}{dt} \tag{3}$$

$$R_p = k[M]^m[I]^n \tag{4}$$

ISSN 2616-5880 Vol. 6, Issue 2: 82-91, DOI: 10.25236/AJMC.2025.060211

where k is the reaction rate constant, m is the monomer concentration indices, and n is the initiator concentration indices. m and n can be obtained from the slope of lgR_p plotted against lg[M] and lg[I], respectively.

Finally, the activation energy, E_a, of each monomer was determined to compare their polymerization activity. According to the above equation and Arrhenius Equation (5), the relationship between polymerization rate and temperature is obtained as shown in Equation (6). Assuming constant monomer and initiator concentrations, the slopes of lnR_p and 1/T can be used to calculate the activation energies of the polymerization reactions for the three monomers.

$$k = \mathrm{A}e^{-\frac{E_a}{RT}} \tag{5}$$

$$lnR_p = \mathrm{lnA} - \frac{E_a}{RT} + mln[M] + nln[I] \tag{6}$$

where k is the reaction rate constant, A is the frequency factor, and R is the gas constant.

Of note, the molecular weight increases with the increase in reactivity ratio. The reactivity ratio (r) can be calculated by Equations 7, 8 and 9:

$$\frac{d[M_1]}{d[M_2]} = \frac{[M_1]}{[M_2]} \times \frac{r_1[M_1] + [M_2]}{r_2[M_2] + [M_1]} \tag{7}$$

$$R - \frac{R}{\rho} = \frac{R^2}{\rho} r_1 - r_2 \tag{8}$$

$$\rho = (1 - C)/C \tag{9}$$

where C is the degree of copolymerization. The cationic determination steps are shown in the Supporting Information.

2.4 Materials characterization.

2.4.1 Structure characterization

Fourier transform infrared spectroscopy. A small amount of the copolymer was applied on disposable potassium bromide tablets, and Fourier transform infrared spectroscopy was performed on a PerKin-Elmer L1600400 infrared spectrometer. The following FTIR settings were used: spectral range 4000 cm^{-1}– 500 cm^{-1}, 64 scans and a resolution of 8. *Nuclear magnetic resonance.* The copolymers were fully dissolved in deuterium water (D_2O) and the analysis run on a 400MHz liquid superconducting nuclear magnetic resonance spectrometer, and the molecular structure of the copolymer products were characterized by ^{1}H NMR.

2.4.2 Determination of relative molecular weight of the polymer

The relative molecular weights of the prepared copolymers were expressed in terms of the intrinsic viscosity [η] and the weight average molecular weight. The intrinsic viscosity [η] of the copolymer was measured by using an ubbelohde viscometer (0.5-0.6 mm) in 1.0 $mol \cdot L^{-1}$ NaCl solution and the polymer concentration was below 1000mg/L, the measurement was conducted at 30±0.05 ℃ (in a water bath). The value of [η] was determined by using a one-point method according to the Solomon-Ciuta formula. The weight-average molecular weight (Mw) of the copolymers were determined with a DAWN HELEOS GPC-MALLS system (Wyatt, USA) using 0.50 mmol/L $NaNO_3$ solution as mobile phase.

2.4.3 Determination of apparent viscosity of the copolymer solutions before and after CO2 response

The apparent viscosity changes of the aqueous copolymer solutions before and after CO_2 treatment is one of the most significant macroscopic properties of CO_2-responsive polymers. A DV2TLV viscometer (Brookfield, U.S.A.) was used to test the apparent viscosity of the solution before and after passing CO_2 (LV-63 rotor was used in both cases, the rotation speed was 60 r/min and the temperature was 25 ℃). The apparent viscosity value of the original solution was first read, and then CO_2 was bubbled through the solution at a rate of 300 mL/min for a duration of 20 min, and the apparent viscosity value was recorded every 5 min. The measurement was repeated three times for each set.

ISSN 2616-5880 Vol. 6, Issue 2: 82-91, DOI: 10.25236/AJMC.2025.060211

2.5 Flocculation method, flocculation performance and mechanism analysis method

The flocculation performance of the copolymerization products was evaluated by the diatomite suspension flocculation test. Deionized water (450 mL) at 25 ℃ was poured into a 500 mL beaker, followed by addition of 5 g diatomite, and the mixture was stirred for 1 min at 200 r/min by using a program-controlled jar test apparatus. The copolymer sample solution prepared in advance was added and stirred for another 5 min. During the mixing process, CO_2 was bubbled in the following ways: (a) the CO_2 was bubbled in the copolymer solution at a rate of 300 mL/min for 20 min in advance, and the protonated polymer solution was added to the diatomite suspension for flocculation; (b) After adding the polymer solution, the CO_2 was bubbled in the diatomite suspension at a rate of 300 mL/min during the flocculation process; (c) the CO_2 was bubbled in the copolymer solution at a rate of 300 mL/min for 20 min in advance. After the protonated polymer solution was added to the diatomite suspension, the CO_2 was bubbled in the diatomite suspension at a rate of 300mL/min during the flocculation process; (d) In the control experiment, the copolymer sample solution was added to the diatomite suspension without addition of CO_2. After stirring, the suspension from the beaker was poured into a 500 mL stopper with a scale, deionized water was added to the 500 mL stopper, the stopper was reversed 2 times, placed on the table and the timer started simultaneously. The height of the settling interface was recorded at 10 s, 20 s, 30 s, 40 s, 50 s, 60 s, 70 s, 80 s, and 90 s intervals. The scatter plot of the settling height H as the vertical coordinate and the settling time as the horizontal coordinate were drawn and the slope of the fitted curve was the settling rate.

After settling for 15 minutes, the supernatant was gently sucked out of the measuring cylinder with a disposable straw and transferred to the test container for determination of turbidity. At the same time, an appropriate amount of supernatant and precipitate were taken into a centrifugal tube, and Zeta potential was measured by a Malvern Zetasizer instrument (Malvern, UK). A sampling spoon was used to pick up a small amount of sediment at the bottom of the measuring cylinder, and it was placed on a slide to observe the microstructure of the sediment floc with a OLYMPUS，BX53，WHN 10X/22 in bright field mode. The remaining sediment was poured into the filter bottle, and the vacuum degree and time were controlled to filter, and the moisture content of the filter cake measured.

The flocculated sediment was poured into a filter bottle covered with filter paper, and the vacuum was controlled to be -0.095 Mpa and the filtration time was 30 s to filter the flocculated sample. The dried petri dish was weighed, the mass of the petri dish and filter paper was noted as w_1; the extracted filter cake was placed in the petri dish and weighed, the mass was noted as w_2; finally, extracted filter cake was placed into the oven set at 105 ℃ for 4 h to constant weight; cooled down, weighed, the mass noted as w_3; and the moisture content of the filter cake was calculated according to Formula (10).

$$w = \frac{w_2 - w_3}{w_2 - w_1} \times 100\% \tag{10}$$

3. Result and Discussion

3.1 Kinetics for co-polymerization of the cationic monomers with DMAEMA

To evaluate the rate of copolymerization between DAC, MAPTAC, DMC and DMAEMA, the changes of conversion rate with time were followed under different monomer concentrations. Figure 2A shows that the copolymerization rate increased with the increase in monomer concentration. The copolymerization rate of DAC with DMAEMA was the highest and that of DMC copolymerized with DMAEMA is the lowest (Figure 2B). On the other hand, the experiments conducted at different initiator concentrations exhibited an increase in the copolymerization rates as a function of increase in the initiator concentration (Figure 2C). The copolymerization rate of DMC with DMAEMA was also the lowest (Figure 2D). The copolymerization rate equations of cationic monomers DAC, MAPTAC and DMC with the CO_2-responsive monomer DMAEMA are as follows: (DAC-DMAEMA:(R_{p5}=$k_5[M]^{4.58}[I]^{0.56}$), MAPTAC-DMAEMA(R_{p6}=$k_6[M]^{4.31}[I]^{0.54}$) and (DMC-DMAEMA (R_{p7}=$k_7[M]^{4.47}[I]^{0.57}$) and were summarized in Table S1.

To obtain the activation energies (E_a) of the copolymerization reactions between DAC, MAPTAC, DMC and DMAEMA, the change of monomer conversion rate as a function of time at different initiation temperatures were tracked (Figure 2E, F). The corresponding E_a of the copolymerization reactions between DAC, MAPTAC, DMC and DMAEMA were found to be 54.36 kJ/mol, 56.94 kJ/mol and 63.82

ISSN 2616-5880 Vol. 6, Issue 2: 82-91, DOI: 10.25236/AJMC.2025.060211

kJ/mol, respectively (Table S2). The above results indicated that the copolymerization reaction between DMC and DMAEMA was lowest.

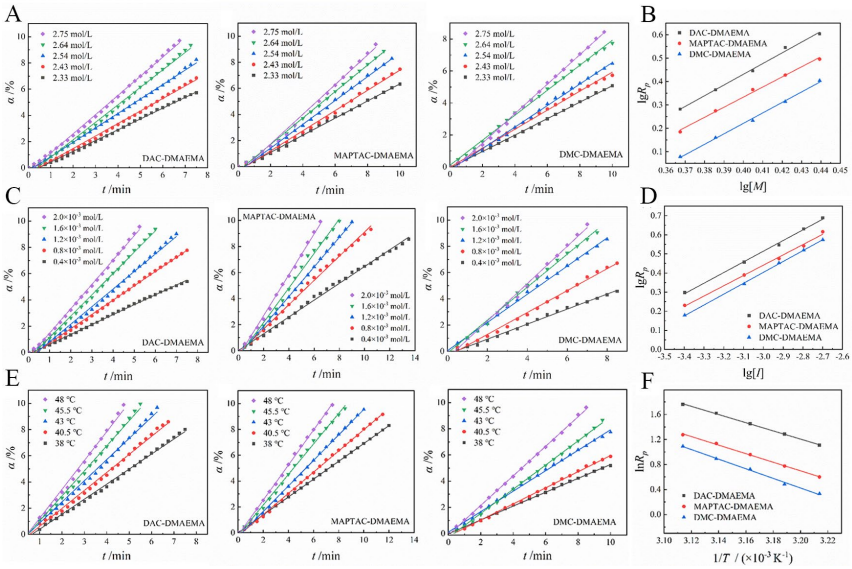

Figure 2. (A) Conversion curves VS time at different monomer concentrations and (B) corresponding fitted curves; (C) Conversion curves VS time at different initiator concentrations and (D) corresponding fitted curves; (E) Conversion curves VS time for different initiation temperatures and (F) corresponding fitted curves

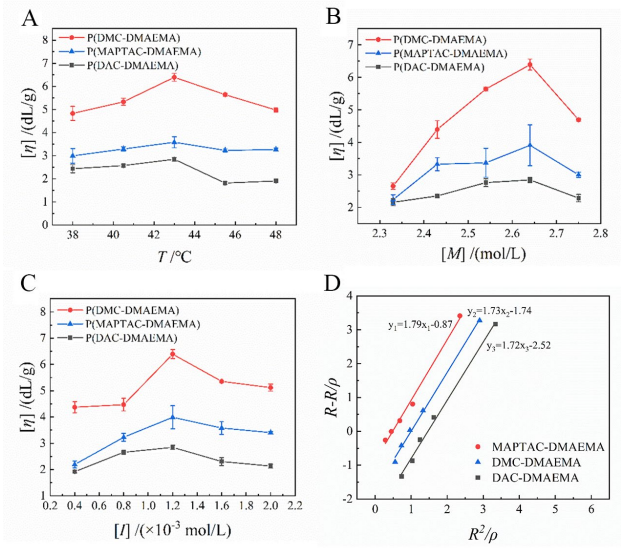

Figure 3. Intrinsic viscosity [η] of P(DAC-DMAEMA), P(MAPTAC-DMAEMA), and P(DMC-DMAEMA) under different (A) initiation temperatures (B) monomer concentrations (C) initiator concentrations and the (D) corresponding fitted lines of the copolymerization reactivity rates.

To assess the copolymerization activity on molecular weight of the copolymers, the relationship between intrinsic viscosity and initiation temperature, monomer concentration and initiator concentration were looked at (Figure 3A-C). The intrinsic viscosity initially increases and then decreases with increase in the initiation temperature, monomer concentration and initiator concentration. Meanwhile, the intrinsic viscosity of P(DMC-DMAEMA) is the highest and that of P(DAC-DMAEMA) is the lowest, indicating the molecular weight of P(DMC-DMAEMA) is maximal (Table S3). The relative reactivities of the two monomers during copolymerization can be determined by the reactivity ratios. As shown in Figure 3D, the formula of the fitting line obtained for the copolymerization of MAPTAC and DMAEMA is $y_1=1.79x_1-0.87$, the slope is 1.79 and the intercept is -0.87. In other words, the reactivity rate of DMAEMA is $r_{11}=1.79$, the reactivity rate of MAPTAC is $r_{12}=0.87$, thus the reactivity rate of DMAEMA was greater than that of MAPTAC. The polymerization activity of DMAEMA monomer was higher than that of MAPTAC. In addition, the reactivity ratios of DMC and DMAEMA were comparable, indicating

ISSN 2616-5880 Vol. 6, Issue 2: 82-91, DOI: 10.25236/AJMC.2025.060211

that they have similar and high copolymerization reaction activity. This may have contributed to the generation of relatively high molecular weight products. Based on the above experimental result, it is necessary to further explore the optimal molar ratio of DMC and DMAEMA copolymerization for effective flocculant with high molecular weight and fast response to CO_2.

The E_a of the copolymerization reaction between DMC and DMAEMA under different molar ratios were examined. The copolymerization rate increased with temperature as seen in Figures 4A-C. Meanwhile, the fitted results exhibited gradual decrease in the copolymerization rate with increase in the molar ratio of DMC and DMAEMA (Figure 4D; Table S4). Furthermore, the differences in the copolymerization rates and relative molecular weights under different monomer molar ratios were quantitatively explained kinetically. The copolymerization rate increased with the increase in monomer concentration (Figure 4E, F). The influence of monomer molar ratio on molecular weights of the copolymers was further explored. With the increase of the trigger temperature, monomer concentration and initiator concentration, the intrinsic viscosity firstly increased and then decreased, and reached the maximum value when the trigger temperature was 43 ℃, monomer concentration was 2.64 mol/L and the initiator concentration was 1.2×10^{-3} mol/L, respectively (Figure 4G-I). Meanwhile, the maximum value of the intrinsic viscosity increased with the increase in the content of DMC, indicating DMC released more free radicals to promote the reaction. As expected, GPC tests showed the highest molecular weight of the P(DMC_3-$DMAEMA_1$) copolymer (Table S5).

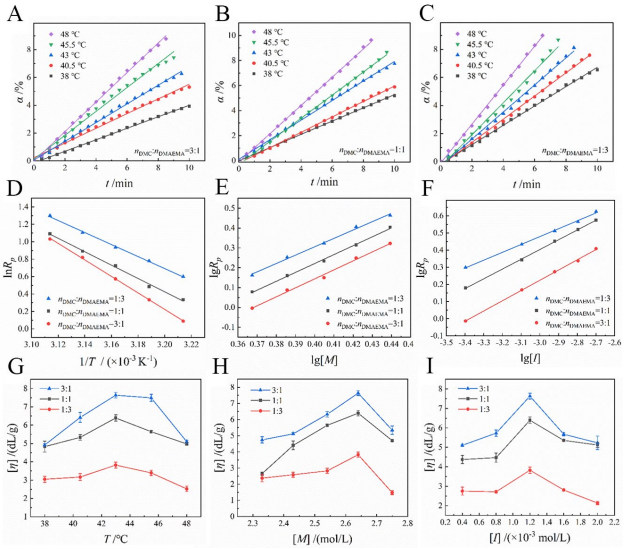

Figure 4. (A-C) Conversion VS time curves for different initiation temperatures under different molar ratios of DMC and DMAEMA (D) corresponding fitted lines; Linearized Arrhenius plots (E) lgR_p and lg[M], (F) lgR_p and lg[I]; Intrinsic viscosity [η] of P(DMC-DMAEMA) with various molar ratio under different (G) initiation temperature, (H) monomer concentration (I) initiator concentration.

3.2 Investigation for structural and CO_2-responsiveness performance

3.2.1 Polymerization mechanism and molecular structure characterization

It can be seen from the Fourier transform infrared (FTIR) spectra that the double bond peaks of the three copolymers all disappear. The methyl peaks of DMAEMA in the P(DAC-DMAEMA) copolymer, observed at 1375 cm^{-1}, were found to increase as compared to the DAC monomer. In the case of P(MAPTAC-DMAEMA) copolymer, the intensity of ester carbonyl group peak (C=O) of DMAEMA was observed at 1720 cm^{-1} increase compared with the MAPTAC monomer (Figure 5A). Furthermore, as shown in Figure 5B, the nuclear magnetic resonance (NMR) spectroscopy demonstrates the double bonds of monomer have been opened, as indicated by disappearance of peaks in the region be and the DAC, DMC, MAPTAC monomers were successfully copolymerized with DMAEMA monomer. To be specific, Peaks a_1(δ=4.09), a_2(δ=4.09) and a_3(δ=3.88) represent the absorption peaks of hydrogen atoms of the -CH_2- group attached to O. The peaks labelled as b_1(δ=3.55), b_2(δ=3.55), b_3(δ=3.40) represent the absorption peaks of hydrogen atoms on the two methyl groups attached to N. The peaks labelled as c_1(δ=3.22), c_2(δ=3.22), c_3(δ=3.19) were assigned to the absorption peaks of hydrogen atoms on the three methyl groups attached to N. The absorption peaks labelled as d_1(δ=2.96), d_2(δ=2.96), d_3(δ=2.79) represent the absorption peaks of hydrogen atoms on the -CH_2- group attached to N. The peaks around

ISSN 2616-5880 Vol. 6, Issue 2: 82-91, DOI: 10.25236/AJMC.2025.060211

e_1(δ=1.90), e_2(δ=1.90), e_3(δ=1.90~2.06) were assigned to the hydrogen absorption peaks connected to C-CH_2-groups. The peaks labelled as f_1(δ=1.08), f_2(δ=1.08), f_3(δ=1.00) are associated with the methyl absorption peaks. The hydrogen absorption peaks on the-CONH-group were observed at g(δ=5.75). These results indicate that all the monomers were completely copolymerized as indicated by absence of double bond peaks in all the cases.

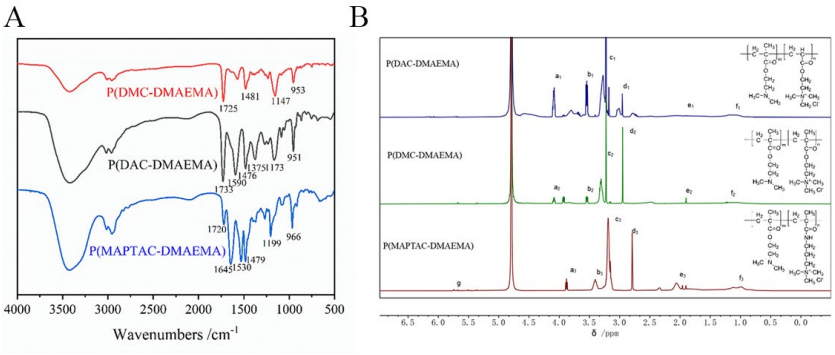

Figure 5. (A) FTIR spectra of different copolymers, (B) NMR spectroscopies of the same copolymers.

3.2.2 Investigation for CO_2-responsiveness performance of copolymers

To verify the practical applications of P(DMC_3-$DMAEMA_1$) copolymer, its performance in solid-liquid separation, the CO_2 response and flocculation performance were assessed. Figure 5A shows the mechanism of solid-liquid separation via employing the CHOPs flocculant. The DMAEMA unit tertiary amine group contains a lone pair of electrons hence has strong electronegativity. After importing CO_2, tertiary amine molecules can be easily protonated with H^+ to form ionic hydrophilic quaternary ammonium salts.

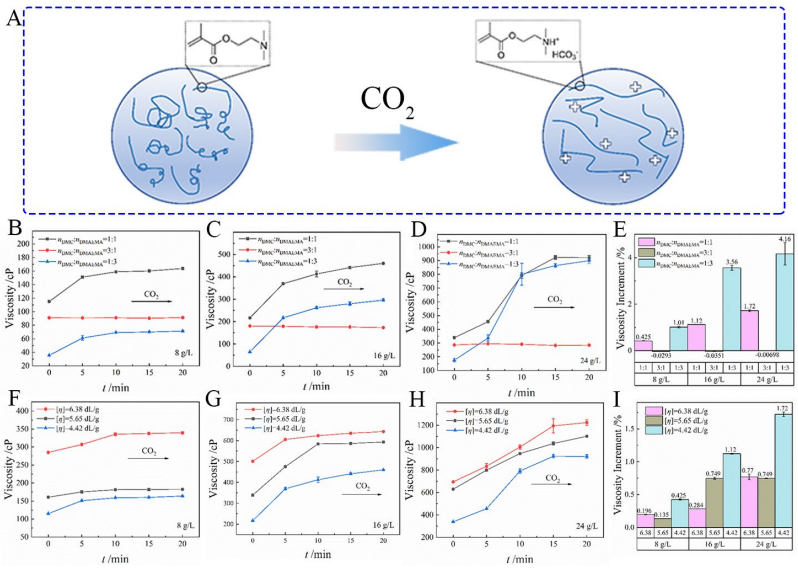

Figure 6. (A) Schematic diagram of response mechanism of CHOP to CO_2. Changes of apparent viscosity of the copolymers produced with different monomer molar ratios before and after CO_2 exposure at copolymer concentrations of (B) 8 g/L, (C) 16 g/L, (D) 24 g/L and (E) the corresponding apparent viscosity as a function of increasing molar ratios. Changes of apparent viscosity of the copolymers with different relative molecular weights before and after CO_2 exposure under copolymer concentrations of (F) 8 g/L, (G) 16 g/L, (H) 24 g/L and (I) corresponding apparent viscosity VS increasing monomer molar ratio.

The CO_2 response performance was characterized by the apparent viscosity of the solution. The apparent viscosity of P(DMC_1-$PDMAEMA_3$) basically increased with the enhanced inlet concentration of CO_2 and the P(DMC_1-$PDMAEMA_3$) copolymer had the most obvious increase in apparent viscosity due to the high CO_2 response monomer content as seen in Figure 6B-E. Meanwhile, the smaller the relative molecular weight of the copolymer in the solution, the greater the increase of apparent viscosity after the introduction of CO_2 and the apparent viscosity changed more drastically with the increase in

ISSN 2616-5880 Vol. 6, Issue 2: 82-91, DOI: 10.25236/AJMC.2025.060211

solution concentration (Figure 6F-I). The results show that the P(DMC_1-$DMAEMA_3$) sample had the potential to be an effective flocculant. With the increase in the copolymer concentration, the apparent viscosity changed more obviously, due to possibly the increase in the concentration hence enabling the tertiary amine group in the copolymer to fully react with CO_2. This was followed by the quaternization of the tertiary amine group by the hydrogen ion from the carbonic acid to form the ionic quaternary ammonium salt. The repulsion forces of charge caused the molecular chains to stretch, resulting in significant increase in the solution viscosity.

4. Conclusions

In summary, the CO_2-responsive cationic copolymers were synthesized via the copolymerization of several cationic monomers (DAC, DMC, and MAPTAC), and CO_2 monomers (DMAEMA). In this study several parameters such as the reaction rate, the activation energy under different CO_2 import modes and relative molecular weight of polymerization products were compared to obtain the CHOPs with the highest relative molecular mass. The monomer content composition was also optimized for effective solid-liquid separation. Especially, the tertiary amine groups of CHOPs could be well-protonated by CO_2, leading to positively charged chains of copolymers. Benefitting from the improved electric neutralization and adsorption bridging effect derived from CO_2-responsiveness, the flocculation of the negatively charged solids in solution can be effectively enhanced, leading to highly efficient solid-liquid separation. Furthermore, the structure-function relationship between CHOPs and CO_2-responsiveness and flocculation ability has been constructed. As a result, the optimized P(DMC-DMAEMA) showed prominent flocculation ability for highly efficient solid-liquid separation. This work will shed light on the actual application of CHOPs in research of solid-liquid separation.

Acknowledgements

This work was supported by the Sichuan Science and Technology Plan Project (Grant No. 2023JDRC0054), the HFIPS Director's Fund (Grant No. YZJJ-GGZX-2022-01).

References

[1] Minudri, D., Mantione, D., Dominguez-Alfaro, A., Moya, S., Maza, E., Bellacanzone, C., Antognazza, M.R.and Mecerreyes, D. (2020) Water Soluble Cationic Poly(3,4-Ethylenedioxythiophene) PEDOT-N as a Versatile Conducting Polymer for Bioelectronics.Advanced Electronic Materials, 6.

[2] Rahmatpour, A., Alijani, N.and Mirkani, A. (2023) Supramolecular self-assembling hydrogel film based on a polymer blend of chitosan/partially hydrolyzed polyacrylamide for removing cationic dye from water.React Funct Polym, 185, 105537.

[3] Skordalou, G., Pachis, K.and Demadis, K.D. (2024) Intrinsic synergy in polymer-induced stabilization of silicic acid by polymeric backbones with cationic and neutral moieties: Implications for "green" scale control in silica-laden industrial waters.Desalination, 577, 117415.

[4] Dou, Y.R., Li, Z., Wang, C.H., Wang, Q.Q., Wang, Z., Wu, Q.H.and Wang, C. (2024) Hydroxyl-functionalized cationic porous organic polymers for efficient enrichment and detection of phenolic endocrine disrupting chemicals in water and snapper.Food Chem, 460, 140587.

[5] Tian, L.C., Zhou, S.Y., Zhao, J.J., Xu, Q.F., Li, N.J., Chen, D.Y., Li, H., He, J.H.and Lu, J.M. (2023) Sulfonate-modified calixarene-based porous organic polymers for electrostatic enhancement and efficient rapid removal of cationic dyes in water.J Hazard Mater, 441, 129873.

[6] Abdiyev, K., Maric, M., Orynbaev, B., Zhursumbaeva, M., Seitkaliyeva, N.and Toktarbay, Z. (2023) A Novel Cationic Polymer Surfactant for Regulation of the Rheological and Biocidal Properties of the Water-Based Drilling Muds.Polymers-Basel, 15, 330.

[7] Lin, W.X., Wu, P.C., Li, R.F., Li, J.H., Cai, Y.M., Yuan, L.H.and Feng, W. (2022) Novel triazine-based cationic covalent organic polymers for highly efficient and selective removal of selenate from contaminated water.J Hazard Mater, 436, 129127.

[8] Li, H.X., Huang, H.L., Yan, X.G., Liu, C.A.X.and Li, L. (2021) A Calix[4]arene-crosslinked polymer for rapid adsorption of cationic dyes in water.Mater Chem Phys, 263, 124295.

[9] Wang, C., Zhu, G.C., Ren, B.Z., Zhang, P.and Hursthouse, A. (2019) A cationic polymer enhanced PAC for the removal of dissolved aquatic organic carbon and organic nitrogen from surface waters.Can J Chem Eng, 97, 955-966.

[10] Zhao, W., Jiao, Y.Z., Gao, R.R., Wu, L.P., Cheng, S.Y., Zhuang, Q., Xie, A.M.and Dong, W. (2020)

ISSN 2616-5880 Vol. 6, Issue 2: 82-91, DOI: 10.25236/AJMC.2025.060211

Sulfonate-grafted conjugated microporous polymers for fast removal of cationic dyes from water.Chem Eng J, 391, 123591.
[11] Jiang, B.X., Zhang, Y.C., Huang, X.D., Kang, T., Severtson, S.J., Wang, W.J.and Liu, P.W. (2019) Tailoring CO-Responsive Polymers and Nanohybrids for Green Chemistry and Processes.Ind Eng Chem Res, 58, 15088-15108.
[12] Zhu, L.P., Powell, S.and Boyes, S. (2015) RAFT polymerization of tertiary amine-based methacrylate pH-responsive monomers for smart MRI contrast agents.Abstr Pap Am Chem S, 249, 1010–1022.
[13] Huang, X.L., Zhang, M.M., Su, X.and Feng, Y.J. (2024) CO2-responsive polymer promoted by polyether to efficient viscosity increase for CO2 plugging.Polymer, 306, 127227.
[14] Li, Y.C., Kong, B.L., Zhang, W.D., Bao, X.N., Jin, J., Wu, X.Y., Guo, Y., Liu, Y.H., Wang, Y.X., He, X.J., Zhang, H., Shen, Z.Q.and She, O. (2020) Field Application of Alkali/Surfactant/Polymer Flood with Novel Mixtures of Anionic/Cationic Surfactants for High-Temperature and High-Water-Cut Mature Sandstone Reservoir.Spe Reserv Eval Eng, 23, 1093-1104.
[15] Hsiao, Y.N., Ilhami, F.B.and Cheng, C.C. (2023) CO-Responsive Water-Soluble Conjugated Polymers as a Multifunctional Fluorescent Probe for Bioimaging Applications.Biomacromolecules, 25, 997-1008.
[16] Wang, B.B., Zhang, Q., Xiong, G., Ding, F., He, Y.K., Ren, B.Y., You, L.X., Fan, X.L., Hardacre, C.and Sun, Y.G. (2019) Bakelite-type anionic microporous organic polymers with high capacity for selective adsorption of cationic dyes from water.Chem Eng J, 366, 404-414.
[17] Liu, X., Ji, B.and Li, A. (2023) Enhancing biolipid production and self-flocculation of Chlorella vulgaris by extracellular polymeric substances from granular sludge with CO2 addition: Microscopic mechanism of microalgae-bacteria symbiosis.Water Res, 236, 119960.
[18] Riabtseva, A., Ellis, S.N., Champagne, P., Jessop, P.G.and Cunningham, M.F. (2021) CO-Responsive Branched Polymers for Forward Osmosis Applications: The Effect of Branching on Draw Solute Properties.Ind Eng Chem Res, 60, 9807-9816.
[19] Zolfaghari, R., Abdullah, L.C., Biak, D.R.A.and Radiman, S. (2019) Cationic Surfactants for Demulsification of Produced Water from Alkaline-Surfactant-Polymer Flooding.Energ Fuel, 33, 115-126.
[20] Shieh, Y.T., Tai, P.Y.and Cheng, C.C. (2019) Polymer nanoparticles with a sensitive CO-responsive hydrophilic/hydrophobic surface.J Polym Sci Pol Chem, 57, 2149-2156.
[21] Yoshida, E. (2019) CO-responsive behavior of polymer giant vesicles supporting hindered amine.Colloid Polym Sci, 297, 661-666.
[22] Fuchs, S., Lichte, D., Dittmar, M., Meier, G., Strutz, H., Behr, A.and Vorholt, A.J. (2017) Tertiary Amines as Ligands in a Four-Step Tandem Reaction of Hydroformylation and Hydrogenation: An Alternative Route to Industrial Diol Monomers.Chemcatchem, 9, 1436-1441.
[23] Nittala, A.K., Gumfekar, S.P.and Soares, J.B.P. (2019) Multifunctional CO-switchable polymers for the flocculation of oil sands tailings.J Appl Polym Sci, 136, 47578.
[24] Ming, A.Q., Li, X.X., Sun, J., Liu, Y.Y., Tian, X.Y., Wang, H., Chen, L., Cao, Y.X.and Yuan, Y. (2024) The comparison of polymerization activity of typical cationic quaternary ammonium salt monomers. Polym Advan Technol, 35, e6277.
[25] Bi, K.Z.and Zhang, Y.J. (2012) Kinetic study of the polymerization of dimethyldiallylammonium chloride and acrylamide.J. Appl. Polym. Sci., 125, 1636-1641.
[26] Jaeger, W., Hahn, M., Wandrey, C., Seehaus, F.and Reinisch, G. (1984) Cyclopolymerization Kinetics of Dimethyl Diallyl Ammonium Chloride.Journal of Macromolecular Science: Part A - Chemistry, 21, 593-614.